HHS Public Access

Author manuscript

Acta Biomater. Author manuscript; available in PMC 2017 November 01.

Published in final edited form as:

Acta Biomater. 2016 November ; 45: 110–120. doi:10.1016/j.actbio.2016.09.006.

Development of peptide-functionalized synthetic hydrogel microarrays for stem cell and tissue engineering applications

Jia Jia[a], **Robert C. Coyle**[a], **Dylan J. Richards**[a], **Christopher Lloyd Berry**[a], **Ryan Walker Barrs**[b], **Joshua Biggs**[a], **C. James Chou**[c], **Thomas C. Trusk**[d], and **Ying Mei**[a,d]

Ying Mei: mei@clemson.edu

[a]Bioengineering Department, Clemson University, Clemson, SC 29634, USA

[b]College of Engineering and Computing, University of South Carolina, Columbia, SC 29208, USA

[c]Department of Drug Discovery and Biomedical Sciences, South Carolina College of Pharmacy, Medical University of South Carolina, Charleston, SC 29425, USA

[d]Department of Regenerative Medicine and Cell Biology, Medical University of South Carolina, Charleston, SC 29425, USA

Abstract

Synthetic polymer microarray technology holds remarkable promise to rapidly identify suitable biomaterials for stem cell and tissue engineering applications. However, most of previous microarrayed synthetic polymers do not possess biological ligands (e.g., peptides) to directly engage cell surface receptors. Here, we report the development of peptide-functionalized hydrogel microarrays based on light-assisted copolymerization of poly(ethylene glycol) diacrylates (PEGDA) and methacrylated-peptides. Using solid-phase peptide/organic synthesis, we developed an efficient route to synthesize methacrylated-peptides. In parallel, we identified PEG hydrogels that effectively inhibit non-specific cell adhesion by using PEGDA-700 (M. W. = 700) as a monomer. The combined use of these chemistries enables the development of a powerful platform to prepare peptide-functionalized PEG hydrogel microarrays. Additionally, we identified a linker composed of 4 glycines to ensure sufficient exposure of the peptide moieties from hydrogel surfaces. Further, we used this system to directly compare cell adhesion abilities of several related RGD peptides: *RGD*, *RGD*S, *RGD*SG and *RGD*SP. Finally, we combined the peptide-functionalized hydrogel technology with bioinformatics to construct a library composed of 12 different RGD peptides, including 6 unexplored RGD peptides, to develop culture substrates for hiPSC-derived cardiomyocytes (hiPSC-CMs), a cell type known for poor adhesion to synthetic substrates. 2 out of 6 unexplored RGD peptides showed substantial activities to support hiPSC-CMs. Among them, PMQKM*RGD*VFSP from laminin β4 subunit was found to support the highest adhesion and sarcomere formation of hiPSC-CMs. With bioinformatics, the peptide-functionalized hydrogel microarrays accelerate the discovery of novel biological ligands to develop biomaterials for stem cell and tissue engineering applications.

Correspondence to: Ying Mei, mei@clemson.edu.

Graphical Abstract

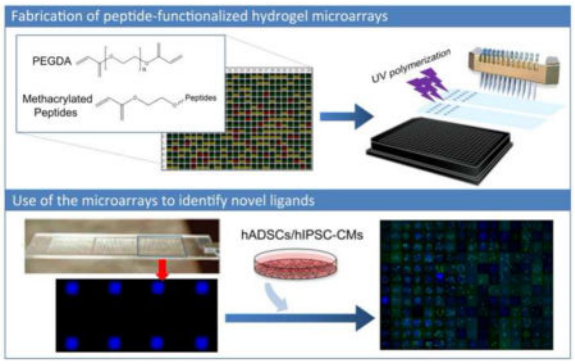

Keywords

peptide-functionalized hydrogel microarray; RGD peptides; Poly(ethylene glycol) hydrogels; methacrylated peptides; human induced pluripotent stem cell-derived cardiomyocytes; cell adhesion

1. Introduction

Polymer array technology has emerged as a powerful tool for the rapid identification of suitable materials for a variety of stem cell and tissue engineering applications [1–7]. To fabricate synthetic polymer microarrays, photopolymerization of (meth)-acrylates has been extensively utilized [4, 8–14]. This is due to their high polymerization rate, as well as the high solubility of (meth)-acrylates in high boiling point organic solvents (e.g., DMF). While this strategy allows for the preparation of synthetic polymers with diversified properties, these polymers usually do not contain biological ligands to directly interact with cell surface receptors (e.g., integrin and growth factor receptors) [7, 15]. The biological functions of these polymers usually depend upon the serum/extracellular matrix (ECM) proteins adsorbed on their surface from pre-conditioning solution and/or cell culture media [5, 10].

To develop substrates capable of interacting with (stem) cell surface receptors in a defined manner, a popular approach is to use functional fragments of ECM proteins (e.g., RGD-peptides) to functionalize the substrates [16–18]. In particular, self-assembled monolayer (SAM) technology has received significant attention as it allows for versatile peptide functionalization strategies [19]. To this end, Kiessling and coworkers prepared thiolated peptides and spotted them onto gold-coated glass slides to prepare peptide-functionalized SAM microarrays [17, 20, 21]. Alternatively, Kilian and coworkers have taken advantage of recent advances in “click” chemistry [22]. They synthesized the alkyne group functionalized peptides and robotically spotted them with azide-terminated alkanethiolate to prepare peptide microarrays. Another approach to prepare peptide-functionalized SAM microarrays has been developed by Murphy and coworkers [18]. They leveraged the carbodiimide catalyzed conjugation reactions between the n-terminal primary amine of peptides and carboxylic acid terminated SAMs to prepare peptide microarrays [19, 23].

In addition to the SAM microarrays, the fabrication of peptide-functionalized hydrogel microarrays has been explored. Unlike with SAMs, hydrogels allow for the easy modulation of the physical properties (e.g., elasticity) of substrates, which has been shown to have controlling effects on (stem) cells [24–26]. For example, Engler and coworkers have shown to influence the differentiation of human mesenchymal stem cells (hMSCs) through the fabrication of hydrogels that closely replicate *in vivo* tissue elasticity [27]. Their results demonstrated that the gels with stiffness similar to muscle elasticity led to myogenic differentiation, while the gels similar to calcified bone led to osteogenic differentiation. To combine the advantages of hydrogels and high-throughput microarray technology, the peptide functionalized hydrogel microarray has been explored. To this end, Hawker and coworkers have developed a versatile synthetic route to prepare peptide-functionalized hydrogel microarrays using thiol-ene chemistry [28]. Despite this progress, the chemistry employed to prepare peptide-functionalized hydrogel microarrays usually involves complicated/inefficient methods of synthesis, limiting their widespread application. We reasoned that through the combination of photopolymerization of (meth)-acrylates and solid-phase peptide/organic synthesis, we could provide a robust approach for the fabrication of peptide-functionalized hydrogel microarrays for numerous stem cell and tissue engineering applications. To the best of our knowledge, no previous researchers have attempted the combined application of these existing chemistries for the methods outlined in this research [18, 28].

Here, we described the development of a platform technology based on light-assisted co-polymerization of poly(ethylene glycol) diacrylates (PEGDA) and methacrylated-peptides to fabricate peptide-functionalized hydrogel microarrays. To this end, we leveraged the high efficiency of solid-phase peptide synthesis and isocyanation chemistry to develop a robust synthetic route for preparing methacrylated-peptides. Due to their high solubility in DMF and high miscibility with low molecular PEGDA, methacrylated-peptides can be effectively incorporated into PEG hydrogels in a ratiometric and homogenous manner. In addition, several parameters were optimized, including the length of the linker between methacrylate functional groups and cell-binding peptide moieties to ensure high accessibility of the peptide functional groups to the cell-surface receptors. The effectiveness of the microarray technology was validated through direct comparison of cell adhesion abilities of highly related RGD peptides: *RGD*, *RGDS*, *RGDSG* and *RGDSP*. To apply the peptide-functionalized hydrogel technology, we constructed a library composed of 12 different RGD peptides to develop synthetic culture substrates for human induced pluripotent stem cell-derived cardiomyocytes (hiPSC-CMs), a cell type known for poor adhesion to synthetic substrates [29]. While 6 of the 12 peptides were found through reported literature, bioinformatic screening of ECM proteins led to the identification of 6 unexplored RGD peptides. Notably, 2 out of 6 unexplored RGD peptides showed substantial affinity to hiPSC-CMs. One of them, PMQKM*RGD*VFSP from laminin β4 subunit, was found to have the highest affinity to hiPSC-CMs. With the support of bioinformatic screening, peptide-functionalized hydrogel microarrays are shown here to be a promising strategy to rapidly identify novel biological ligands for the development of functional biomaterials for stem cell and tissue engineering applications.

2. Material and methods

2.1 Materials and instruments

All chemicals used for this study were purchased from Sigma-Aldrich (St. Louis, MO) unless otherwise stated. Microarray spotting pins (946MP9B) were purchased from Arrayit Corporation (Sunnyvale, CA). A custom designed microarrayer was assembled and produced by BioDot (Irvine, CA). The liquid chromatography-mass spectrometer (LC-MS) system used is Thermo Fisher LCQ Fleet^{tm} Ion Trap Mass Spectrometer.

2.2 Bioinformatics-assisted ECM protein screening

Bioinformatics-assisted ECM protein screening for highly conserved sequences was performed using the following database: UniProt database, which is supported by European Bioinformatics Institute (EMBI-EBI), the SIB Swiss Institute of Bioinformatics, and the Protein Information Resource (PIR). The specific sequence of each ECM protein/ECM protein subunit was collected from mammalian species, including human, mouse, rat, chimpanzee, horse, sheep, rabbit, bovine, guinea pig, cat and dog. The protein alignment was achieved by using the tool of Clustal Omega [30–32] from EMBL-EBI. The algorithm is described by J. Söding [33]. The highly conserved sequences among different species have been selected out as demonstrated in Figure S4.

2.3 Monomer preparation and array fabrication

Synthesis and characterization of methacrylated peptides—Peptides used in this work were synthesized by solid phase peptide synthesis (SPPS). The SPPS was conducted using the standard procedure described in Novabiochem peptide synthesis manual. To prepare methyacrylated peptides, 2-isocyanatoethyl methacrylate (3 equivalent (eq) dissolved in DMF) was used to react with the terminal amine group of the peptide chain (1 eq) before they were cleaved from the resin. This solid-phase isocyanation chemistry was first reported by Lee Ayres *et. al.* [34]. All the methacrylated peptides prepared in this study were purified by using a Combiflash® purification system (RediSep Rf) in Reversed Phase format using C18 Columns (Teledyne Isco, Lincoln, NE) running a solvent gradient from 100% H_2O to 100% acetonitrile in 15~20 minutes. The peptides were eluted from the column at approximately 70% acetonitrile/30% H_2O. The purified peptides were subsequently characterized by LC-MS.

Microarray Fabrication—Methacrylated peptides were dissolved in DMF at pre-designated ratios and mixed with PEGDA (containing 1% DMPA as initiator) (DMF solution of methacrylated peptide: PEGDA = 1:1 (v/v)) and then transferred into a 384 well plate for microarray fabrication. The microarrays were printed in a humid Ar-atmosphere on epoxy monolayer-coated glass slides (Xenopore XENOSLIDE E, Hawthorne, NJ) that were first dip-coated in 4 v/v% poly(hydroxyethyl methacrylate) (i.e., poly(HEMA)) using a customized microarrayer (Biodot). Spots were polymerized via 10 s exposure to long wave UV using a XX-15L UV bench lamp (365 nm) (UVP LLC, Upland, CA), dried at <50 mtorr for at least 7 days. Before use, the chips were sterilized by UV for 30 min for each side, and then washed with PBS twice for 15 min to remove residual monomer or solvent. Additional information to prepare the microarrays for different applications is provided below.

PEGDA selection—Three commercially available PEGDA (M. W. = 250, 575, 700) were selected and mixed at the designated ratios to produce the hydrogel microarrays (Figure S2). To determine their abilities to inhibit unspecific cell adhesion, human adipose-derived stem cells (hADSCs) were seeded on the array and cultured for 12 hours. They were then fixed and stained with DAPI (1:1000 in DPBS) for cell number counting and phalloidin (1:200 in DPBS) for F-actin to estimate cell spreading.

The effects of glycine linker length and the comparison of *RGD*, *RGDS*, *RGDSG* and *RGDSP* peptides—The methacrylated peptides used in these experiments are shown in Figure 5A and 6A. PEGDA and methacrylated peptides were mixed at varied peptide concentrations (i.e., 0.5, 1, 3, 6, 9, 12 and 15 mM) to prepare microarrayed hydrogels with different peptide concentrations. hADSCs were seeded onto the array and cultured for 12 hours. They were then fixed and stained with DAPI (1:1000 in DPBS) for cell number counting and phalloidin (1:200 in DPBS) for F-actin to estimate cell spreading.

Screening RGD peptides for hiPSC-CM adhesion and quantification of sarcomere formation—The methacrylate peptides used in this experiment are shown in Figure 7B. PEGDA and methacrylated peptides were mixed at one fixed peptide concentration (15 mM) to prepare microarrayed hydrogels with a constant peptide concentration. hiPSC-CMs (human induced pluripotent stem cell-derived cardiomyocytes from Cellular Dynamics International, Madison, WI, USA) were seeded onto the microarray and cultured for 3 days to facilitate the formation of sarcomere structures. hiPSC-CMs were stained with DAPI to approximate cell number and phalloidin for F-actin to estimate cell spreading. Sarcomere structure was examined by using immunofluorecence microscopy.

Briefly, hiPSC-CMs on the microarray were fixed with 4% PFA solution and blocked by 10% goat serum. After incubated with mouse anti-alpha sarcomeric actinin antibody (Abcam, Cambridge, UK) and rabbit anti-troponin I antibody (Santa Cruz, Dallas, TX) at a dilution ratio of 1: 200 in PBS (with 0.1% Triton-100X) at room temperature for 1 hr, the microarrays were stained with the secondary antibodies (Alexa-488 goat anti-mouse IgG and Alexa-647 goat anti-rabbit IgG) at a dilution ratio of 1:200 in PBS (with 0.1% Triton-100X). Subsequently, the microarrays are stained with DAPI (1:1000 in DPBS) for nuclear counting. The fluorescently stained microarrays were imaged with a TCS SP5 AOBS laser scanning confocal microscope (Leica Microsystems, Inc., Exton, PA). Z-stacked Images collected from the microarray were analyzed by using the ImageJ (National Institutes of Health) for semi-quantitative analysis of the expression level of alpha sarcomeric actinin of hiPSC-CMs on the microarrays. The sarcomeric actinin expression level of hiPSC-CMs on each hydrogel spot was determined by the total fluorescence intensities of sarcomeric actinin staining divided by the total cell number on the hydrogel spot, which was then normalized to the blank PEG-700 hydrogel spots. The fluorescence intensities of sarcomeric actinin staining on each hydrogel spot were obtained by taking the sum of the green (sarcomeric actinin staining) pixels (i.e., fluorescence area coverage) through the total thickness of the Z-stacked images [35].

2.4 Cell culture

hADSC culture—hADSCs (Lonza, Basel, Switzerland) were used to study cell attachment for the hydrogel array. The cells were cultured in low glucose Dulbecco's modified Eagle's medium with 10% fetal bovine serum and 1% penicillin-streptomycin, 1% glutamine and 1% antimycin (Gibco Life Technologies, Grand Island, NY). At >80% confluency, cells were detached using trypLE Express (Gibco Life Technologies) and passaged. All experiments were conducted using passage 5 (P5) hADSCs. The cells were seeded along with culture media onto the hydrogel microarrays. After 12 hours culture, the cells were fixed and stained to examine the cell attachments on each spot. hADSCs were stained with DAPI (1:1000 in DPBS) in order to approximate cell number. Cell spreading was visualized using phalloidin (1:200 in DPBS) staining.

hiPSC-CMs culture—hiPSC-derived cardiomyocytes (iCell Cardiomyocytes, Cellular Dynamics International, Madison, WI, USA) were cultured according to the manufacturer's protocol. Briefly, hiPSC-derived cardiomyocytes were plated on 0.1% gelatin coated 6-well plates in iCell Cardiomyocytes Plating Medium (Cellular Dynamics International) at a density of about 3×10^5 to 4.0×10^5 cells/well and incubated at 37 °C in 5% CO_2 for 4 days. Two days after plating, the plating medium was removed and replaced with 4 mL of iCell Cardiomyocytes Maintenance Medium (Cellular Dynamics International). After 4 days of monolayer pre-culture, cells were detached using trypLE Express (Gibco Life Technologies, Grand Island, NY) and seeded along with culture media on the hydrogel microarrays. Cells were culture for 3 days to allow the hiPSC-CMs to develop sarcomere structures. hiPSC-CMs were stained with DAPI (1:1000 in DPBS) to approximate cell attachment number and phalloidin (1:200 in DPBS) for F-actin to estimate cell spreading. Sarcomere structures were visualized using sarcomere actinin and troponin-I staining as described above.

2.5 Statistical analysis

The results were shown in the mean ± standard derivation (SD) and analyzed using Sigmaplot and Excel statistical software.

3. Results and discussion

Figure 1 shows a general strategy for the fabrication of peptide-functionalized PEG microarrays for stem cell and tissue engineering applications. To fabricate the microarrays, nanoliters of PEGDA and methacrylated-peptides have been robotically deposited onto poly(HEMA) coated glass slides and photo-polymerized in situ. This approach is chosen due to the high polymerization rate of photopolymerization [36] and the high solubility of methacrylated-peptides in DMF [37]. In addition, peptide-functionalized PEG hydrogels have been extensively employed in stem cell and tissue engineering applications [38–40]. This makes it possible to quickly translate the screening results into design principles for the improved fabrication of 2D culture substrates and 3D scaffolds.

Figure 2 demonstrates a general procedure to prepare methacrylated-peptides. After solid-phase peptide synthesis, 2-isocyanatoethyl methacrylate was used to react with the terminal

amine of the peptides in order to conjugate methacrylate groups [34]. As the conjugation reaction step was right after peptide synthesis on the solid-phase, this route allows for the preparation of methacrylated-peptides from virtually any peptides. Further, this solid-phase conjugation reaction has been proven very effective and efficient. The synthesis of methacrylated GGGG*RGD*SP (i.e., MethG4*RGD*SP) peptide is provided as an example (Figure S1A and S1B).

To provide a low cell adhesion background for peptide screening, PEGDA of different molecular weights were screened to generate the non-fouling PEG hydrogel substrates. To this end, three commercially available low molecular weight PEGDA: PEGDA-250 (molecular weight, M. W. = 250), PEGDA-575 (M. W. = 575), PEGDA-700 (M. W. = 700), have been used to fabricate an 8 x 8 microarray to screen for formulations that can resist non-specific cell adhesion. After seeding human adipose-derived stem cells (hADSCs) onto the hydrogel microarray, every spot composed of PEGDA-250 showed extensive cell adhesion. While the spots made by PEGDA-575 were right at the threshold to resist cell attachment (only 1 or 2 cells/spot), no cell attachment was recorded for those made of PEGDA-700 (Figure S2). The differences in cell adhesion can be attributed to the ethylene glycol chain length of the PEGDA, as the longer ethyl glycol chain provides significantly enhanced chain flexibility to resist protein adsorption and cell adhesion [41, 42]. Since the spots prepared from the PEGDA-700 showed high resistance to non-specific cell adhesion, PEGDA-700 was selected to co-polymerize with methacrylated-peptides to prepare peptide-functionalized PEG hydrogel microarrays.

To confirm the effective incorporation of methacrylated-peptides and the homogenous distribution of the peptide moieties within the PEG hydrogels, we synthesized fluorescently labeled methacrylated-peptides (i.e., MethGD(coumarin)GG*RGD*SP) as shown in Figure 3 and prepared fluorescently-labeled-peptide functionalized PEG hydrogels (Figure 3A-C, S1C). Figure 3B shows a linear relationship between the concentration of the MethGD(coumarin)GG*RGD*SP in the printing solution and fluorescence intensity of the hydrogel spots. This clearly indicates peptide concentration within each spot is determined by methacrylated-peptide concentration in the printing solution. Notably, Figure 3C also shows a homogenous distribution of peptides within the hydrogels. The ability to control peptide concentration, as well as their homogeneous distribution within hydrogel spots, allows us to develop peptide-functionalized hydrogel to direct (stem) cells.

To validate the functions of the peptide moieties on the hydrogels, we synthesized a methacrylated-peptide containing a cell adhesive moiety (G_4*RGD*SP) and its scrambled sequence (G_4RDGSP) (Figure S1A, D). The methacrylated-peptides were then co-polymerized with PEGDA-700 to prepare PEG hydrogel spots functionalized with cell adhesive *RGD* peptides or the scrambled RDG peptide. As shown in the Figure 4, PEG hydrogels modified with a high concentration of (15 mM) *RGD*-peptide were able to effectively promote adhesion of hADSCs (Figure 4, right), while no cell adhesion was found on the scrambled peptide (RDG) functionalized PEG hydrogels (Figure 4, middle) [43]. These results indicate the function of peptides is retained during the microarray fabrication process.

The length of the linker between peptide moiety and hydrogel surface has been shown to significantly influence peptide activities and further affect cell behavior [44]. While there is one ethylene glycol group between methacrylate and the cell-binding peptide moiety, it may not be sufficient to ensure the exposure of the peptides on the hydrogel surface for cell recognition. Enlightened by the idea of using a 4-glycine linker to extend the RGD peptide from hydrogel surface [45, 46], we designed and synthesized methacrylated-*RGD*SP-peptides with no glycine linker (Meth*RGD*SP), 2 glycine linker (MethG_2*RGD*SP), 4 glycine linker (MethG_4*RGD*SP) and 6 glycine linker (MethG_6*RGD*SP), as listed in Figure 5A. The microarrays composed with these peptides have been fabricated and hADSCs were seeded onto the array. Sigmoidal relationships between the number of attached cells and peptide concentration were found for all of these RGD peptides (Figure 5B) [10]. Given the sigmoidal relationship, small changes in peptide concentration can result in large shifts in cell attachment numbers at lower peptide concentrations. To reduce variation in the high throughput analysis, the saturated (maximum) number of attached cells has been used to examine the effects of changing glycine linker length (Figure 5C). MethG_4*RGD*SP and MethG_6*RGD*SP showed similar saturation numbers for attached cells (Figures 5B and 5C). They are about one-fold higher than the saturation number of attached cells of Meth*RGD*SP and MethG_2*RGD*SP. These results indicate that longer linkers improved the exposure of the peptides on the hydrogel surface. Also, the similar cell attachment between MethG_4*RGD*SP and MethG_6*RGD*SP suggested that 4 glycine provides sufficient length as a linker between the methacrylate and peptide components for our system. Therefore, further experiments were performed using peptides modified with the four-glycine linker.

RGD peptides have been widely used to improve cell adhesion by immobilizing them onto the surface of 2D substrates and 3D scaffolds [45–47]. In the literature, a series of sequentially similar RGD peptides have been utilized, such as *RGD*, *RGD*S, *RGD*SG and *RDG*SP [48–50]. Although it is well acknowledged that the amino acid(s) surrounding the key tri-peptides (RGD) can significantly influence the binding interactions between RGD peptides and integrin [51], little research has been done directly comparing the cell adhesion ability of *RGD*, *RGD*S, *RGD*SG and *RGD*SP [23]. Our peptide-functionalized PEG hydrogel system can allow for a direct comparison of cell adhesion ability of these RGD peptides. To this end, we fabricated a hydrogel microarray composed of *RGD*, *RGD*S, *RGD*SG and *RGD*SP (Figure 6A) with different concentrations (0.5mM-15mM). The analyses were conducted after seeding the hADSCs onto the fabricated microarray. Again, a sigmoidal relationship was identified between the number of attached cells and peptide concentration for each of the RGD peptides (Figure 6B). *RGD*SP showed at least a one-fold increase in the saturated number of attached cells when compared with *RGD*, *RGD*S and *RGD*SG, while *RGD*, *RGD*S, and *RGD*SG showed similar saturation numbers for cell attachment (Figure 6C). The improved cell adhesion of *RGD*SP peptides can be attributed to the rigid structure of proline (P), which can reduce the flexibility of the peptide chain and increase its affinity towards corresponding integrin subunits [51, 52].

While the use of saturated cell binding criterion allows for reduced variation during high throughput synthesis and analysis, changes in the sub-threshold peptide concentrations can lead to different cell functions, including differentiation, and provides an effective means to manipulate stem cells [53–57]. Here, as a functional indicator, the extent of cell spreading

was observed to parallel the shifts in the cell attachment at different peptide concentrations, shown with *RGD*SG (0.5mM-15mM) in Figure S3. Specifically, less spreading was observed at low peptide concentrations (0.5 and 1mM), consistent with previous literature suggesting the ligand density is able to influence (stem) cell morphology [53, 55, 58]. In this manuscript, we focused on high-density peptides due to the current lack of high affinity ligands for biomaterials development [59–61].

The newly developed peptide-functionalized hydrogel microarray will allow us to rapidly identify novel peptides to functionalize biomaterials for numerous stem cell and tissue engineering applications. To this end, we used this technology to screen adhesion peptides for human induced pluripotent stem cell-derived cardiomyocytes (hiPSC-CMs). While hiPSC-CMs hold remarkable promise as a cell source to treat cardiovascular diseases [62–65], they have been reported as having poor adhesion on synthetic substrates [66]. hiPSC-CMs express integrin α_3, α_5, α_6, α_7, α_V, β_1 and β_5 [66]. Given the high affinity of RGD peptides to integrin $\alpha_V\beta_5$ [51] [67], we reasoned that RGD peptide functionalization can improve the binding affinity of PEG hydrogel substrates to hiPSC-CMs. To rapidly identify RGD peptide candidates with the potential of high affinity to hiPSC-CMs, we utilized an online bioinformatics tool (UniProtKB database) to screen and align the whole sequence of fibronectin, vitronectin and laminin through multiple species. We selected 12 different RGD peptides (Figure 7B) to construct a PEG hydrogel microarray functionalized with these peptides. The candidates include: 1) 6 RGD peptides that have been reported to improve cell adhesion, such as those selected from laminin-α1 [68], laminin-α5 [69], fibronectin [70] and vitronectin [71], and 2) 6 RGD peptides that have not been studied, but have been shown to be highly conserved sequences among the different mammalian species (Figure S4). The highly conserved RGD sequences among different mammalian species indicate their importance for certain fundamental functions (e.g. cell adhesion/integrin binding). One RGD peptide (PQVT*RGD*VFTMP) from vitronectin, has been included in the microarrays as a control as they were shown to support adhesion of hiPSC-CMs [71].

hiPSC-CMs were seeded onto the RGD peptides functionalized PEG hydrogel microarrays to examine the abilities of different RGD peptides for the enhanced cell adhesion. The cell adhesion response varied among the hydrogels: ~50% of RGD peptides could not support adhesion of hiPSC-CMs (Figure 7A-a, 7A-b, Figure S5 top), some RGD peptides (e.g., PQVT*RGD*VFTMP and SETQ*RGD*VFVP) support moderate cell adhesion (Figure 7A-c, Figure S5 middle), and PMQKM*RGD*VFSP (laminin β4 chain) showed the greatest ability to promote hiPSC-CM adhesion and sarcomere formation, a critical step for cardiomyocytes maturation (Figure 7A-d and Figure S5 bottom). The screening results have been validated with 18 replicates. It is worthwhile to note 2 out of 6 unexplored RGD peptides (PMQKM*RGD*VFSP, DAVKQLQAAERGDA) have shown substantial activities to support hiPSC-CM adhesion. This supports our hypothesis that highly conserved RGD peptide sequences among different species indicate their importance in functions (e.g., cell adhesion/integrin binding). This highlights the power of the combination of the microarray technology we developed here and the bioinformatics tool we utilized to rapidly identify novel biological ligands for the development of functional biomaterials for stem cell and tissue engineering applications. To the best of our knowledge, the highest cell adhesive peptide identified in this study, PMQKM*RGD*VFSP from laminin β4 subunit, has not been

recognized as being a cell-adhesive peptide. Our current research includes the utilization of this novel RGD peptide from laminin β4 subunit to prepare 3D scaffolds for cardiac tissue engineering applications. Notably, the RGD peptide from vitronectin (PQVT*RGD*VFTMP) showed moderate binding affinity for hiPSC-CMs (Figure 7C, D), which could explain a previous report that hiPSC-CMs detach from synthetic substrates during the cardiac differentiation process [66].

We also examined the effects of the peptide sequences on sarcomere formation of hiPSC-CMs using sarcomeric actinin staining (Figure 7A, E), as sarcomeres are structural and functional units for cardiomyocytes contractions. The trend of alpha sarcomeric actinin expression per cell was found similar to that of cell adhesion (i.e., the affinities of peptide ligands). This can be attributed to that the high affinity peptide ligands can provide sufficient support for cardiomyocyte contractions and facilitate sarcomere formation. Consistent with the cell adhesion results, the RGD peptide from laminin β4 subunit supported hiPSC-CMs with the highest sarcomeric actinin expression. With the assistance from confocal microscope, the detailed sarcomere structures were revealed (Figure S6). This data suggests the RGD peptide from laminin β4 subunit can effectively support hiPSC-CM attachment, spreading and contractile structure development. These results are in agreement with a recent report that showed integrin binding is essential for hiPSC-CM maturation [72].

4. Conclusion

Recent advances in stem cell and tissue engineering strategies highlight an unmet need to rapidly identify suitable biomaterials for cell-specific applications. Here we developed a peptide-functionalized PEG hydrogel microarray based on light-assisted, co-polymerizations between poly(ethylene glycol) diacrylates (PEGDA) and methacrylated-peptides. By leveraging solid-phase peptide/organic synthesis, methacrylate-peptides can be synthesized from virtually any peptide sequences. When combined with a cell-adhesion resistant hydrogel derived from PEGDA-700, we have developed a framework for fabricating peptide-functionalized hydrogel microarrays. In addition, we demonstrated the homogenous distribution of peptides within the hydrogels, and identified a linker composed of 4 glycines that can ensure sufficient exposure for the peptide moieties on the hydrogel surface. Further, we used this system to directly compare the cell adhesion abilities of several highly related RGD peptides, *RGD*, *RGD*S, *RGD*SG and *RGD*SP. Lastly, we combined peptide-functionalized microarray technology with bioinformatics to identify novel biological ligands with high affinity to hiPSC-CMs, a cell type known for poor adhesion to synthetic substrates. Among 6 unexplored RGD peptides, 2 peptides showed substantial affinity to hiPSC-CMs. PMQKM*RGD*VFSP from laminin β4 subunit, a peptide that had not previously been recognized as being cell adhesive, was found to have the highest affinity to hiPSC-CMs and the most developed sarcomere structures.

The technology we developed here can allow for the rapid identification of biological ligands for stem cell and tissue engineering application. As peptide-functionalized PEG hydrogels are widely used in stem cell and tissue engineering applications, the screening results could be quickly translated to 2D substrates and 3D scaffold fabrication. Although PEGDA-700 was used to fabricate hydrogel to resist non-specific cell adhesion in this study,

clearly, PEGDA-700 can be replaced with another non-fouling hydrogel-precursors (e.g., PEGDA 3400, methacrylated hyaluronic acids) to vary the bulk properties (e.g., stiffness) of the hydrogel substrates. Our next step is to fabricate hydrogel microarrays that can cover the entire physiological/pathological range of stiffnesses. The ability to rapidly screen the combined effects of biological ligands and mechanical properties on (stem) cells can dramatically accelerate the advancement of the fundamental understanding of the interaction (stem) cell activity and biomaterials. This would further contribute to the development of biomaterial genomics through Big Data analytics [4, 5].

Finally, the peptide-functionalized hydrogel microarrays developed here can find many applications in biomedical-related fields beyond stem cell and tissue engineering. For instance, Morgan and coworkers have utilized synthetic polymer microarrays to identify materials able to resist the adhesion of bacteria for medical devices applications [73]. We can envision that peptide-functionalized hydrogel microarrays will be used to develop anti-infectious substrates, given the wide application of the peptides and hydrogels for designing anti-infectious materials [74, 75].

Supplementary Material

Refer to Web version on PubMed Central for supplementary material.

Acknowledgments

The authors would like to thank the financial support from the National Institutes of Health (8P20 GM103444, U54 GM104941), the startup funds from Clemson University, and the National Science Foundation (NSF - EPS-0903795). D.J.R is supported by the NIH Cardiovascular Training Grant (T32 HL007260). We would like to thank Dr. Ander Hook, Dr. Morgan Alexander and Biodot for their support in the design and fabrication of the microarrayer. This study used the services of the Morphology, Imaging, and Instrumentation Core, which is supported by NIH-NIGMS P30 GM103342 to the South Carolina COBRE for Developmentally Based Cardiovascular Diseases.

References

1. Mei Y. Microarrayed Materials for Stem Cells. Materials today. 2012:15.
2. Fernandes TG, Diogo MM, Clark DS, Dordick JS, Cabral JM. High-throughput cellular microarray platforms: applications in drug discovery, toxicology and stem cell research. Trends in biotechnology. 2009; 27:342–9. [PubMed: 19398140]
3. Yliperttula M, Chung BG, Navaladi A, Manbachi A, Urtti A. High-throughput screening of cell responses to biomaterials. European journal of pharmaceutical sciences : official journal of the European Federation for Pharmaceutical Sciences. 2008; 35:151–60. [PubMed: 18586092]
4. Mei Y, Saha K, Bogatyrev SR, Yang J, Hook AL, Kalcioglu ZI, Cho SW, Mitalipova M, Pyzocha N, Rojas F, Van Vliet KJ, Davies MC, Alexander MR, Langer R, Jaenisch R, Anderson DG. Combinatorial development of biomaterials for clonal growth of human pluripotent stem cells. Nature materials. 2010; 9:768–78. [PubMed: 20729850]
5. Celiz AD, Smith JG, Langer R, Anderson DG, Winkler DA, Barrett DA, Davies MC, Young LE, Denning C, Alexander MR. Materials for stem cell factories of the future. Nature materials. 2014; 13:570–9. [PubMed: 24845996]
6. Anderson DG, Levenberg S, Langer R. Nanoliter-scale synthesis of arrayed biomaterials and application to human embryonic stem cells. Nature biotechnology. 2004; 22:863–6.
7. Coyle R, Jia J, Mei Y. Polymer microarray technology for stem cell engineering. Acta biomaterialia. 2015

8. Gauvin R, Chen YC, Lee JW, Soman P, Zorlutuna P, Nichol JW, Bae H, Chen S, Khademhosseini A. Microfabrication of complex porous tissue engineering scaffolds using 3D projection stereolithography. Biomaterials. 2012; 33:3824–34. [PubMed: 22365811]

9. Lewis KJ, Anseth KS. Hydrogel scaffolds to study cell biology in four dimensions. MRS bulletin / Materials Research Society. 2013; 38:260–8.

10. Mei Y, Gerecht S, Taylor M, Urquhart AJ, Bogatyrev SR, Cho S-W, Davies MC, Alexander MR, Langer RS, Anderson DG. Mapping the Interactions among Biomaterials, Adsorbed Proteins, and Human Embryonic Stem Cells. Advanced Materials. 2009; 21:2781–6.

11. Yang J, Mei Y, Hook AL, Taylor M, Urquhart AJ, Bogatyrev SR, Langer R, Anderson DG, Davies MC, Alexander MR. Polymer surface functionalities that control human embryoid body cell adhesion revealed by high throughput surface characterization of combinatorial material microarrays. Biomaterials. 2010; 31:8827–38. [PubMed: 20832108]

12. Celiz AD, Smith JG, Patel AK, Langer R, Anderson DG, Barrett DA, Young LE, Davies MC, Denning C, Alexander MR. Chemically diverse polymer microarrays and high throughput surface characterisation: a method for discovery of materials for stem cell culture. Biomaterials science. 2014; 2:1604–11. [PubMed: 25328672]

13. Celiz AD, Smith JG, Patel AK, Hook AL, Rajamohan D, George VT, Flatt L, Patel MJ, Epa VC, Singh T, Langer R, Anderson DG, Allen ND, Hay DC, Winkler DA, Barrett DA, Davies MC, Young LE, Denning C, Alexander MR. Discovery of a Novel Polymer for Human Pluripotent Stem Cell Expansion and Multilineage Differentiation. Adv Mater. 2015

14. Anderson DG, Putnam D, Lavik EB, Mahmood TA, Langer R. Biomaterial microarrays: rapid, microscale screening of polymer-cell interaction. Biomaterials. 2005; 26:4892–7. [PubMed: 15763269]

15. Ifkovits JL, Burdick JA. Review: photopolymerizable and degradable biomaterials for tissue engineering applications. Tissue engineering. 2007; 13:2369–85. [PubMed: 17658993]

16. Koepsel JT, Brown PT, Loveland SG, Li WJ, Murphy WL. Combinatorial screening of chemically defined human mesenchymal stem cell culture substrates. Journal of materials chemistry. 2012; 22:19474–81. [PubMed: 23976824]

17. Wrighton PJ, Klim JR, Hernandez BA, Koonce CH, Kamp TJ, Kiessling LL. Signals from the surface modulate differentiation of human pluripotent stem cells through glycosaminoglycans and integrins. Proceedings of the National Academy of Sciences of the United States of America. 2014; 111:18126–31. [PubMed: 25422477]

18. Nguyen EH, Zanotelli MR, Schwartz MP, Murphy WL. Differential effects of cell adhesion, modulus and VEGFR-2 inhibition on capillary network formation in synthetic hydrogel arrays. Biomaterials. 2014; 35:2149–61. [PubMed: 24332391]

19. Love, J Christopher; LAE; Kriebel, Jennah K.; Nuzzo, Ralph G.; Whitesides, George M. Self-Assembled Monolayers of Thiolates on Metals as a Form of Nanotechnology. Chem Rev. 2005; 105:1103–69. [PubMed: 15826011]

20. Derda R, Li L, Orner BP, Lewis RL, Thomson JA, Kiessling LL. Defined substrates for human embryonic stem cell growth identified from surface arrays. ACS chemical biology. 2007; 2:347–55. [PubMed: 17480050]

21. Klim JR, Li L, Wrighton PJ, Piekarczyk MS, Kiessling LL. A defined glycosaminoglycan-binding substratum for human pluripotent stem cells. Nature methods. 2010; 7:989–94. [PubMed: 21076418]

22. Zhang D, Kilian KA. Peptide microarrays for the discovery of bioactive surfaces that guide cellular processes: a single step azide–alkyne “click” chemistry approach. J Mater Chem B. 2014; 2:4280.

23. Coyle R, Jia J, Mei Y. Polymer microarray technology for stem cell engineering. Acta biomaterialia. 2016; 34:60–72. [PubMed: 26497624]

24. Wang H, Tibbitt MW, Langer SJ, Leinwand LA, Anseth KS. Hydrogels preserve native phenotypes of valvular fibroblasts through an elasticity-regulated PI3K/AKT pathway. Proceedings of the National Academy of Sciences of the United States of America. 2013; 110:19336–41. [PubMed: 24218588]

25. Wen JH, Vincent LG, Fuhrmann A, Choi YS, Hribar KC, Taylor-Weiner H, Chen S, Engler AJ. Interplay of matrix stiffness and protein tethering in stem cell differentiation. Nature materials. 2014
26. Elosegui-Artola A, Bazellieres E, Allen MD, Andreu I, Oria R, Sunyer R, Gomm JJ, Marshall JF, Jones JL, Trepat X, Roca-Cusachs P. Rigidity sensing and adaptation through regulation of integrin types. Nature materials. 2014; 13:631–7. [PubMed: 24793358]
27. Engler AJ, Sen S, Sweeney HL, Discher DE. Matrix elasticity directs stem cell lineage specification. Cell. 2006; 126:677–89. [PubMed: 16923388]
28. Gupta N, Lin BF, Campos LM, Dimitriou MD, Hikita ST, Treat ND, Tirrell MV, Clegg DO, Kramer EJ, Hawker CJ. A versatile approach to high-throughput microarrays using thiol-ene chemistry. Nature chemistry. 2010; 2:138–45.
29. Mordwinkin NM, Burridge PW, Wu JC. A review of human pluripotent stem cell-derived cardiomyocytes for high-throughput drug discovery, cardiotoxicity screening, and publication standards. Journal of cardiovascular translational research. 2013; 6:22–30. [PubMed: 23229562]
30. Sievers F, Wilm A, Dineen D, Gibson TJ, Karplus K, Li W, Lopez R, McWilliam H, Remmert M, Söding J. Fast, scalable generation of high-quality protein multiple sequence alignments using Clustal Omega. Molecular systems biology. 2011:7.
31. Goujon M, McWilliam H, Li W, Valentin F, Squizzato S, Paern J, Lopez R. A new bioinformatics analysis tools framework at EMBL–EBI. Nucleic acids research. 2010; 38:W695–W9. [PubMed: 20439314]
32. McWilliam H, Li W, Uludag M, Squizzato S, Park YM, Buso N, Cowley AP, Lopez R. Analysis tool web services from the EMBL-EBI. Nucleic acids research. 2013; 41:W597–W600. [PubMed: 23671338]
33. Söding J. Protein homology detection by HMM–HMM comparison. Bioinformatics. 2005; 21:951–60. [PubMed: 15531603]
34. Ayres L, Vos MR, Adams PHM, Shklyarevskiy IO, van Hest JC. Elastin-based side-chain polymers synthesized by ATRP. Macromolecules. 2003; 36:5967–73.
35. Tong Z, Sant S, Khademhosseini A, Jia X. Controlling the fibroblastic differentiation of mesenchymal stem cells via the combination of fibrous scaffolds and connective tissue growth factor. Tissue Engineering Part A. 2011; 17:2773–85. [PubMed: 21689062]
36. Cook WD. Photopolymerization kinetics of dimethacrylates using the camphorquinone/amine initiator system. Polymer. 1992; 33:600–9.
37. Pechar M, Pola R. The coiled coil motif in polymer drug delivery systems. Biotechnology advances. 2013; 31:90–6. [PubMed: 22266376]
38. DeForest CA, Anseth KS. Cytocompatible click-based hydrogels with dynamically tunable properties through orthogonal photoconjugation and photocleavage reactions. Nature chemistry. 2011; 3:925–31.
39. Burdick JA, Anseth KS. Photoencapsulation of osteoblasts in injectable RGD-modified PEG hydrogels for bone tissue engineering. Biomaterials. 2002; 23:4315–23. [PubMed: 12219821]
40. Zhu J. Bioactive modification of poly(ethylene glycol) hydrogels for tissue engineering. Biomaterials. 2010; 31:4639–56. [PubMed: 20303169]
41. Tziampazis E, Kohn J, Moghe PV. PEG-variant biomaterials as selectively adhesive protein templates: model surfaces for controlled cell adhesion and migration. Biomaterials. 2000; 21:511–20. [PubMed: 10674816]
42. Jeon SI, Lee JH, Andrade JD, GDGP. Protein—surface interactions in the presence of polyethylene oxide- I. Simplified theory. J Colloid Interface Sci. 1990; 142:149–58.
43. Park YD, Tirelli N, Hubbell JA. Photopolymerized hyaluronic acid-based hydrogels and interpenetrating networks. Biomaterials. 2003; 24:893–900. [PubMed: 12504509]
44. Hern DL, Hubbell JA. Incorporation of adhesion peptides into nonadhesive hydrogels useful for tissue resurfacing. Journal of biomedical materials research. 1998; 39:266–76. [PubMed: 9457557]
45. Bouhadir KH, Lee KY, Alsberg E, Damm KL, Anderson KW, Mooney DJ. Degradation of partially oxidized alginate and its potential application for tissue engineering. Biotechnology progress. 2001; 17:945–50. [PubMed: 11587588]

46. Simmons CA, Alsberg E, Hsiong S, Kim WJ, Mooney DJ. Dual growth factor delivery and controlled scaffold degradation enhance in vivo bone formation by transplanted bone marrow stromal cells. Bone. 2004; 35:562–9. [PubMed: 15268909]
47. Jia J, Richards DJ, Pollard S, Tan Y, Rodriguez J, Visconti RP, Trusk TC, Yost MJ, Yao H, Markwald RR, Mei Y. Engineering alginate as bioink for bioprinting. Acta biomaterialia. 2014; 10:4323–31. [PubMed: 24998183]
48. Hirano Y, Kando Y, Hayashi T, Goto K, Nakajima A. Synthesis and cell attachment activity of bioactive oligopeptides: RGD, RGDS, RGDV, and RGDT. Journal of biomedical materials research. 1991; 25:1523–34. [PubMed: 1724445]
49. Chueh BH, Zheng Y, Torisawa YS, Hsiao AY, Ge C, Hsiong S, Huebsch N, Franceschi R, Mooney DJ, Takayama S. Patterning alginate hydrogels using light-directed release of caged calcium in a microfluidic device. Biomedical microdevices. 2010; 12:145–51. [PubMed: 19830565]
50. Ruf A, Schlenk RF, Maras A, Morgenstern E, Patscheke H. Contact-induced neutrophil activation by platelets in human cell suspensions and whole blood. Blood. 1992; 80:1238–46. [PubMed: 1355374]
51. D'Souza SE, Ginsberg MH, Plow EF. Arginyl-glycyl-aspartic acid (RGD): a cell adhesion motif. Trends in biochemical sciences. 1991; 16:246–50. [PubMed: 1926332]
52. Ruoslahti E. RGD and other recognition sequences for integrins. Annual review of cell and developmental biology. 1996; 12:697–715.
53. Garcia AJ, Keselowsky BG. Biomimetic surfaces for control of cell adhesion to facilitate bone formation. Crit Rev Eukaryot Gene Expr. 2002; 12:151–62. [PubMed: 12434928]
54. Rowley JA, Mooney DJ. Alginate type and RGD density control myoblast phenotype. Journal of biomedical materials research. 2002; 60:217–23. [PubMed: 11857427]
55. Mei Y, Elliott JT, Smith JR, Langenbach KJ, Wu T, Xu C, Beers KL, Amis EJ, Henderson L. Gradient substrate assembly for quantifying cellular response to biomaterials. Journal of biomedical materials research Part A. 2006; 79:974–88. [PubMed: 16948143]
56. Dalby MJ, Gadegaard N, Oreffo RO. Harnessing nanotopography and integrin-matrix interactions to influence stem cell fate. Nature materials. 2014; 13:558–69. [PubMed: 24845995]
57. Kilian KA, Mrksich M. Directing stem cell fate by controlling the affinity and density of ligand-receptor interactions at the biomaterials interface. Angewandte Chemie. 2012; 51:4891–5. [PubMed: 22505230]
58. Chaudhuri O, Mooney DJ. Stem-cell differentiation: Anchoring cell-fate cues. Nature materials. 2012; 11:568–9. [PubMed: 22717486]
59. Rice JJ, Martino MM, De Laporte L, Tortelli F, Briquez PS, Hubbell JA. Engineering the regenerative microenvironment with biomaterials. Advanced healthcare materials. 2013; 2:57–71. [PubMed: 23184739]
60. Collier JH, Segura T. Evolving the use of peptides as components of biomaterials. Biomaterials. 2011; 32:4198–204. [PubMed: 21515167]
61. Richards D, Jia J, Yost M, Markwald R, Mei Y. 3D Bioprinting for Vascularized Tissue Fabrication. Ann Biomed Eng. 2016
62. Thomson JA, Itskovitz-Eldor J, Shapiro SS, Waknitz MA, Swiergiel JJ, Marshall VS, Jones JM. Embryonic stem cell lines derived from human blastocysts. Science. 1998; 282:1145–7. [PubMed: 9804556]
63. Sallam K, Kodo K, Wu JC. Modeling Inherited Cardiac Disorders. Circulation Journal. 2014; 78:784–94. [PubMed: 24632794]
64. Laflamme MA, Chen KY, Naumova AV, Muskheli V, Fugate JA, Dupras SK, Reinecke H, Xu C, Hassanipour M, Police S, O'Sullivan C, Collins L, Chen Y, Minami E, Gill EA, Ueno S, Yuan C, Gold J, Murry CE. Cardiomyocytes derived from human embryonic stem cells in pro-survival factors enhance function of infarcted rat hearts. Nature biotechnology. 2007; 25:1015–24.
65. Chong JJ, Yang X, Don CW, Minami E, Liu YW, Weyers JJ, Mahoney WM, Van Biber B, Palpant NJ, Gantz JA, Fugate JA, Muskheli V, Gough GM, Vogel KW, Astley CA, Hotchkiss CE, Baldessari A, Pabon L, Reinecke H, Gill EA, Nelson V, Kiem HP, Laflamme MA, Murry CE. Human embryonic-stem-cell-derived cardiomyocytes regenerate non-human primate hearts. Nature. 2014

66. Burridge PW, Matsa E, Shukla P, Lin ZC, Churko JM, Ebert AD, Lan F, Diecke S, Huber B, Mordwinkin NM, Plews JR, Abilez OJ, Cui B, Gold JD, Wu JC. Chemically defined generation of human cardiomyocytes. Nature methods. 2014; 11:855–60. [PubMed: 24930130]

67. Fondevila C, Shen XD, Moore C, Busuttil RW, Coito AJ. Cyclic RGD peptides with high affinity for alpha5beta1 integrin protect genetically fat Zucker rat livers from cold ischemia/reperfusion injury. Transplantation proceedings. 2005; 37:1679–81. [PubMed: 15919428]

68. Weeks BS, Kopp JB, Horikoshi S, Cannon FB, Garrett M, Kleinman HK, Klotman PE. Adult and fetal human mesangial cells interact with specific laminin domains. The American journal of physiology. 1991; 261:F688–95. [PubMed: 1928380]

69. Sasaki T, Timpl R. Domain IVa of laminin alpha5 chain is cell-adhesive and binds beta1 and alphaVbeta3 integrins through Arg-Gly-Asp. FEBS letters. 2001; 509:181–5. [PubMed: 11741585]

70. Yamada T, Matsushima M, Inaka K, Ohkubo T, Uyeda A, Maeda T, Titani K, Sekiguchi K, Kikuchi M. Structural and functional analyses of the Arg-Gly-Asp sequence introduced into human lysozyme. The Journal of biological chemistry. 1993; 268:10588–92. [PubMed: 8486712]

71. Melkoumian Z, Weber JL, Weber DM, Fadeev AG, Zhou Y, Dolley-Sonneville P, Yang J, Qiu L, Priest CA, Shogbon C, Martin AW, Nelson J, West P, Beltzer JP, Pal S, Brandenberger R. Synthetic peptide-acrylate surfaces for long-term self-renewal and cardiomyocyte differentiation of human embryonic stem cells. Nature biotechnology. 2010; 28:606–10.

72. Herron TJ, Rocha AM, Campbell KF, Ponce-Balbuena D, Willis BC, Guerrero-Serna G, Liu Q, Klos M, Musa H, Zarzoso M, Bizy A, Furness J, Anumonwo J, Mironov S, Jalife J. Extracellular Matrix-Mediated Maturation of Human Pluripotent Stem Cell-Derived Cardiac Monolayer Structure and Electrophysiological Function. Circulation Arrhythmia and electrophysiology. 2016:9.

73. Hook AL, Chang CY, Yang J, Luckett J, Cockayne A, Atkinson S, Mei Y, Bayston R, Irvine DJ, Langer R, Anderson DG, Williams P, Davies MC, Alexander MR. Combinatorial discovery of polymers resistant to bacterial attachment. Nature biotechnology. 2012; 30:868–75.

74. Zumbuehl A, Ferreira L, Kuhn D, Astashkina A, Long L, Yeo Y, Iaconis T, Ghannoum M, Fink GR, Langer R, Kohane DS. Antifungal hydrogels. Proceedings of the National Academy of Sciences of the United States of America. 2007; 104:12994–8. [PubMed: 17664427]

75. Loose C, Jensen K, Rigoutsos I, Stephanopoulos G. A linguistic model for the rational design of antimicrobial peptides. Nature. 2006; 443:867–9. [PubMed: 17051220]

Statement of Significance

In this manuscript, we described the development of a robust approach to prepare peptide-functionalized synthetic hydrogel microarrays. Combined with bioinformatics, this technology enables us to rapidly identify novel biological ligands for the development of the next generation of functional biomaterials for stem cell and tissue engineering applications.

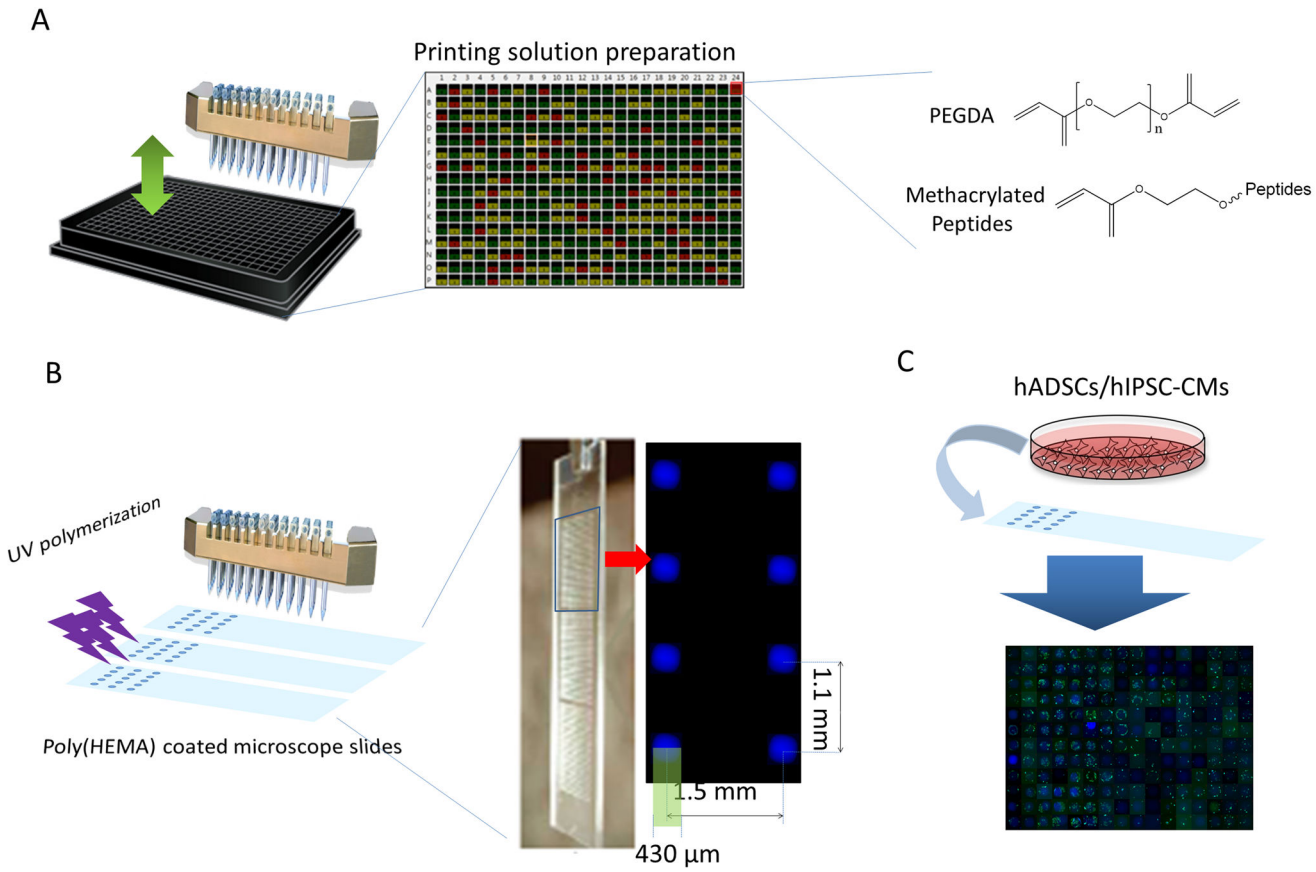

Figure 1.

Schematic representation of fabrication of peptide-functionalized PEG hydrogel microarrays. A. The printing solutions composed of PEGDA monomer and various methacrylated peptides were prepared in a 384-well plate. B. The printing solutions were placed onto poly(HEMA) coated microscope slides with a customized microarrayer and polymerized by UV under Argon protection to prepare peptide-functionalized PEG hydrogel spots. Eight hydrogel spots in a microarray were shown to present the dimension of the hydrogel spots and the distance between the hydrogel spots. C. High throughput analysis of cellular activities after cell seeding onto the microarray.

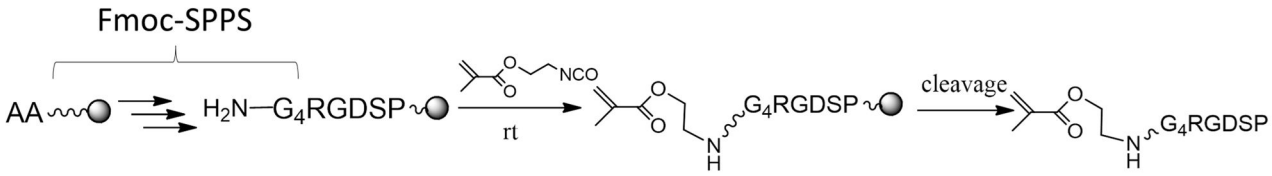

Figure 2.

The methacrylated peptides are prepared by conjugating 2-isocyanatoethyl methacrylate with the terminal amine of the peptides on the solid-phase.

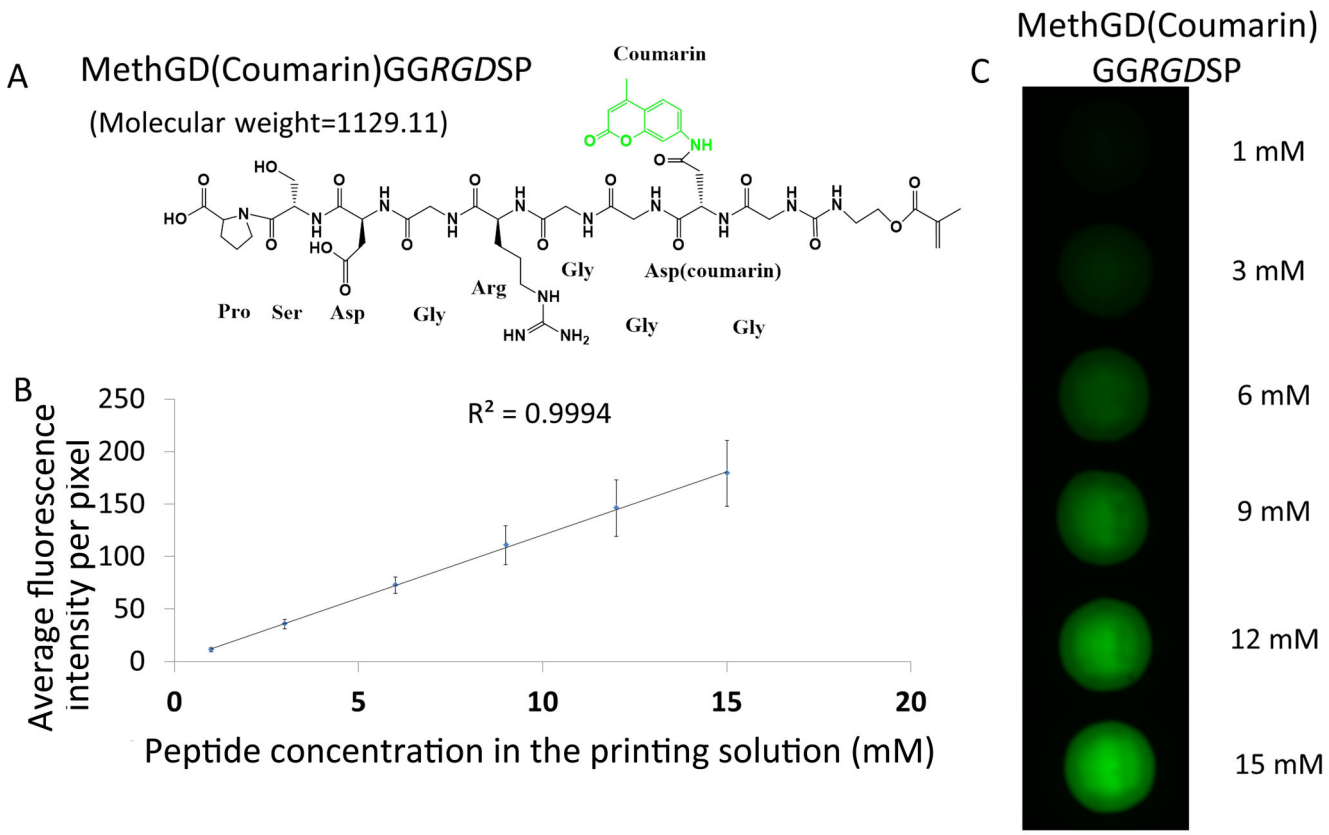

Figure 3.

Validation of peptide concentration and its homogenous distribution within the hydrogel spots. A. Chemical structure and molecular weight of fluorescently labeled MethGD(coumarin)GG*RGD*SP peptides. B. The linear relationship between the peptide concentration and average intensity of each pixel on the fluorescent pictures of the spots. C. Fluorescent pictures of spots with MethGD(coumarin)GG*RGD*SP of various concentrations (varying from 1 to 15 mM).

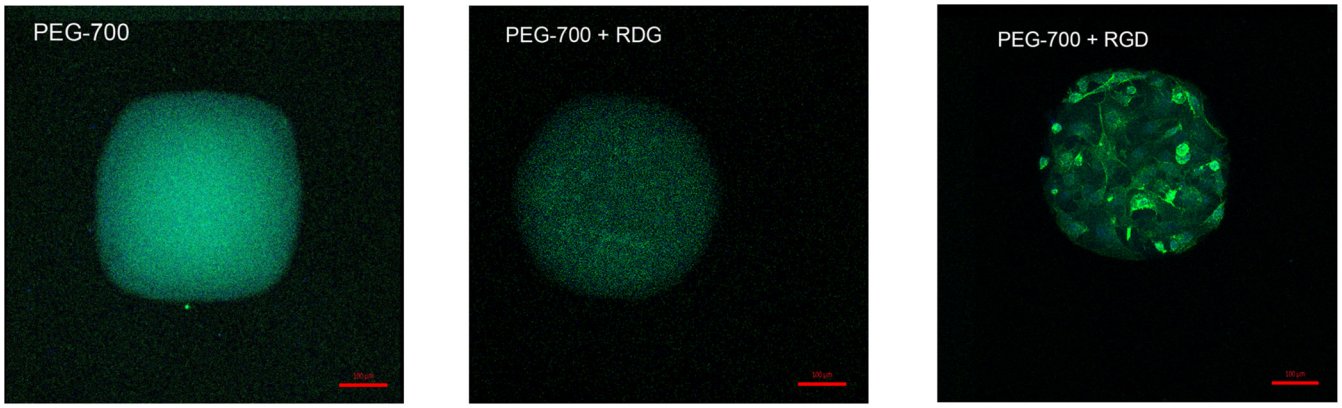

Figure 4.

Functional validation of the peptide moieties on the hydrogels. The representative fluorescent images of blank PEGDA-700 hydrogels (left), RDGSP functionalized PEGDA-700 hydrogels (middle) and *RGD*SP functionalized PEGDA-700 hydrogels (right) after hADSC seeding (blue: DAPI, green: phalloidin, scale bar = 100 μm).

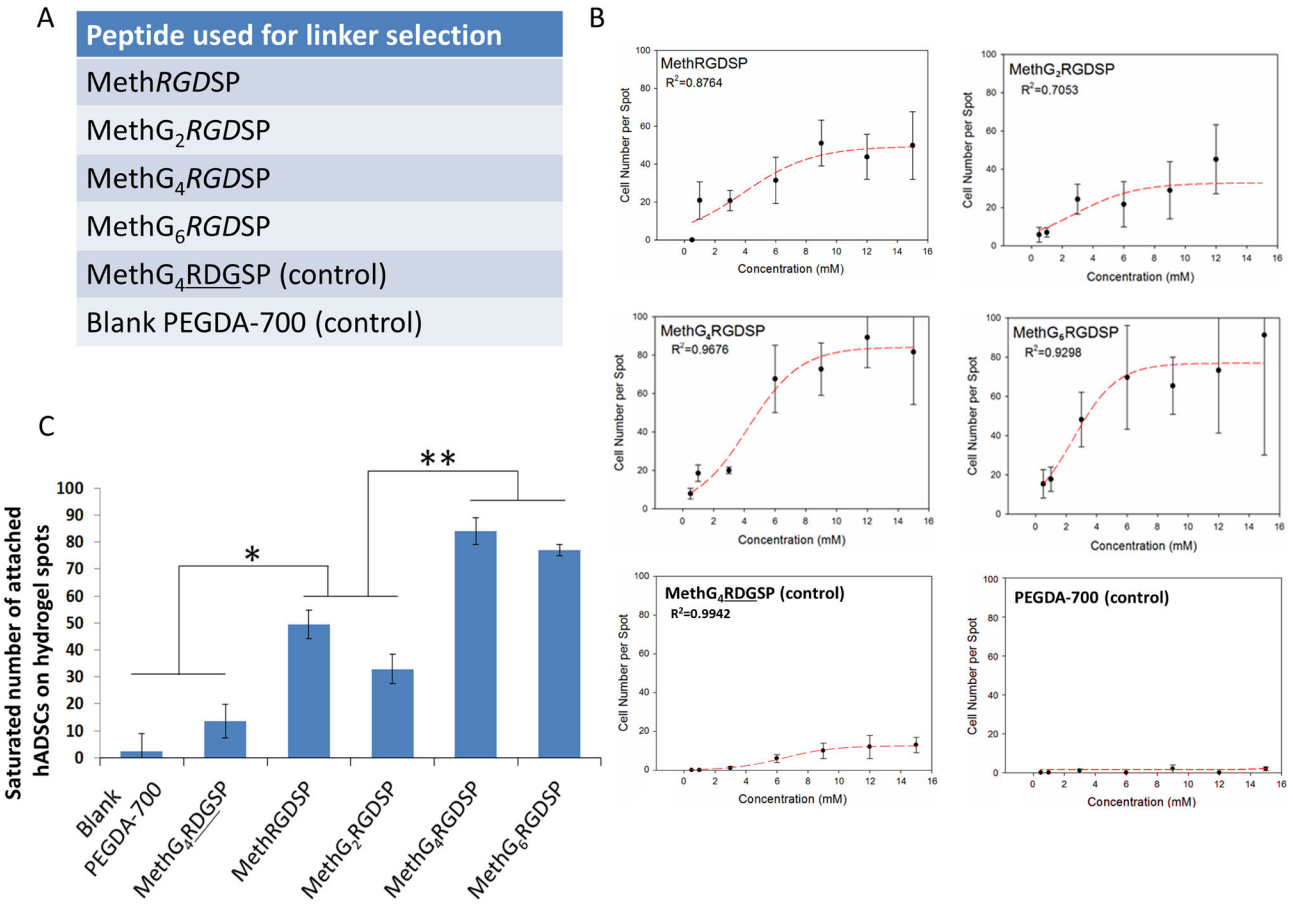

Figure 5.

Selection of a suitable linker to ensure the exposure of peptide moieties on PEG hydrogel surface. A. A list of peptides used for the linker selection: *RGD*SP peptides fused with zero/two/four/six glycine linker, RDGSP and no peptide functionalization (blank PEGDA-700 hydrogel) have been employed as controls. B. Effects of peptide concentration on the average number of the attached hADSCs on the hydrogel spots and the sigmoidal curve-fits. C. Effects of glycine linker length on the saturated number of attached hADSCs on the hydrogel spots. All values are mean ± SD. Asterisk denotes significant difference between blank PEGDA-700 hydrogels, MethG4RDGSP and Meth*RGD*SP, MethG2*RGD*SP. Double asterisk denotes significant difference between Meth*RGD*SP, MethG2*RGD*SP and MethG4*RGD*SP, MethG6*RGD*SP.

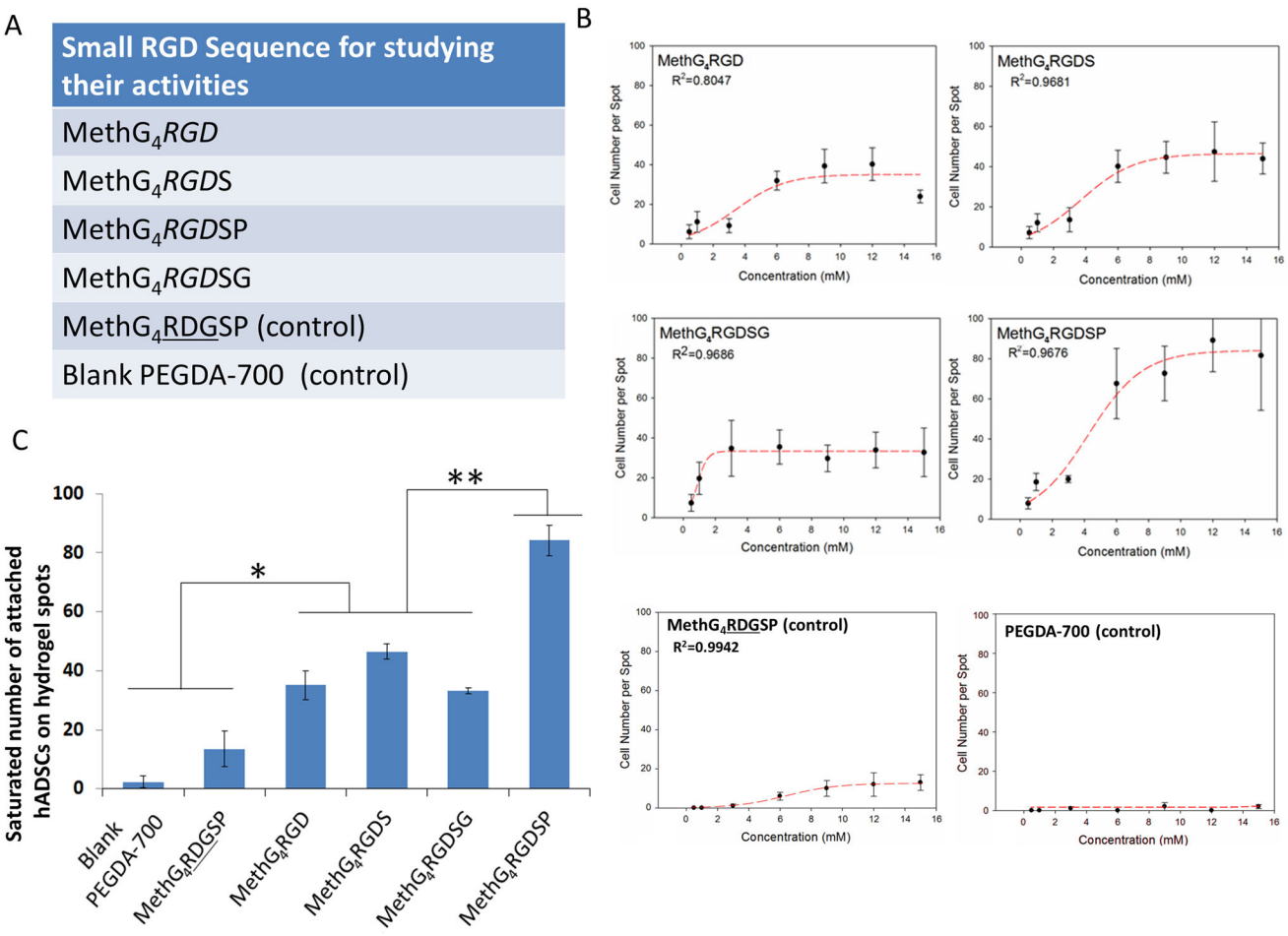

Figure 6.

The activities of various short RGD peptides for hADSCs attachment. A. A list of peptides used in this experiment. B. Effects of peptide concentration on the average number of attached hADSCs on the hydrogel spots and the sigmoidal curve-fits. C. The saturated number of attached hADSCs on the hydrogel spots functionalized with different short RGD peptides. All values are mean ± SD. Asterisk denotes significant difference between blank PEGDA-700 hydrogel, MethG$_4$RDGSP and MethG$_4$*RGD*, MethG$_4$*RGD*S, MethG$_4$*RGD*SG. Double asterisk denotes significant difference between MethG$_4$*RGD*, MethG$_4$*RGD*S, MethG$_4$*RGD*SG and MethG$_4$*RGD*SP.

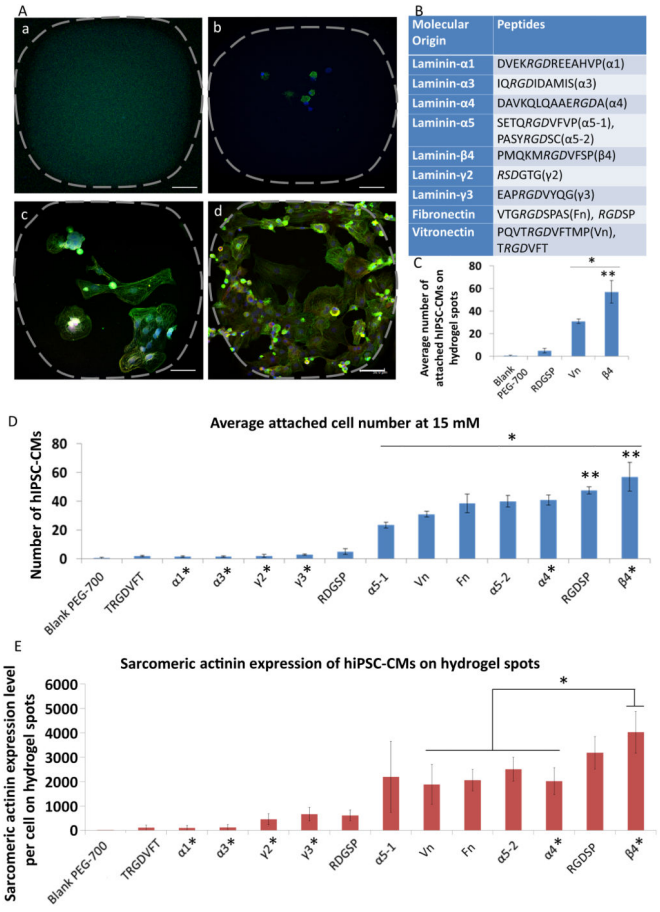

Figure 7.

hiPSC-CM adhesion and sarcomere formation on hydrogel microarrays. A. The representative pictures of hiPSC-CMs on PEG hydrogel spots functionalized with different RGD peptides (blue: DAPI; green: sarcomere actinin; red: Troponin-I, scale bar = 50 μm): a. PEG hydrogel spots functionalized with RGD peptides that could not support adhesion of hiPSC-CMs. b. PEG hydrogel spots functionalized with peptides that can support minimal cell adhesion. c. PEG hydrogel spots functionalized with peptides that can moderately support cell adhesion d. PEG hydrogel spots functionalized with RGD peptides that can effectively promote hiPSC-CM adhesion and sarcomere formation, a critical step for cardiomyocyte maturation. B. A list of RGD peptides used in this experiment and their molecular origin. C. The average number of attached hiPSC-CMs on the hydrogel spots functionalized with RGD peptides from laminin β4 chain, RGD peptides from Vn and two controls (i.e., blank PEGDA-700 hydrogel and RDGSP peptide functionalized hydrogel). All values are mean ± SD. Asterisk denotes significant difference between RGD peptide from laminin β4 chain, RGD peptide from Vn and two control groups. Double asterisk denotes significant difference between laminin β4 RGD peptides and Vn RGD peptide. D. The average number of attached hiPSC-CMs on PEG hydrogel spots functionalized with all different RGD sequences. Asterisk denotes significant difference between the “active” RGD peptides and “inactive” RGD peptides plus two control groups. Double asterisk denotes significant difference between laminin β4 RGD peptides, RGDSP and other RGD peptides

from ECM proteins. Peptides labeled with asterisk were identified through bioinformatics screening. E. The sarcomere actinin expressions of hiPSC-CMs (pixels per cell) cultured on the hydrogel spots. Asterisk denotes significant difference between RGD peptide from laminin β4 chain and RGD peptides from Vn, Fn, α5-2, α4. Peptides labeled with asterisk were identified through bioinformatics screening.